Title

Sequential deletion of CD63 identifies topologically distinct scaffolds for surface engineering of exosomes in living human cells

Journal

Nanoscale, 12(22)

ISSN

2040-3364

Authors

Curley, Natalie
Levy, Daniel
Do, Mai Anh
et al.

Publication Date

2020-06-11

DOI

10.1039/d0nr00362j

Peer reviewed

HHS Public Access

Author manuscript

Nanoscale. Author manuscript; available in PMC 2021 June 11.

Published in final edited form as:

Nanoscale. 2020 June 11; 12(22): 12014–12026. doi:10.1039/d0nr00362j.

Sequential deletion of CD63 identifies topologically distinct scaffolds for surface engineering of exosomes in living human cells

Natalie Curley[1], **Daniel Levy**[1], **Mai Anh Do**[1], **Annie Brown**[1], **Zachary Stickney**[1], **Gerard Marriott**[2,*], **Biao Lu**[1,*]

[1]Department of Bioengineering, Santa Clara University, 500 El Camino Real, Santa Clara, CA 95053, USA.

[2]Department of Bioengineering, University of California at Berkeley, Berkeley, CA 94720, USA

Abstract

Exosomes are cell-derived extracellular vesicles that have great potential in the field of nano-medicine. However, a fundamental challenge in the engineering of exosomes is the design of biocompatible molecular scaffolds on their surface to enable cell targeting and therapeutic functions. CD63 is a hallmark protein of natural exosomes that is highly enriched on the external surface of the membrane. We have already described the engineering of CD63 as a molecular scaffold in order to introduce cell-targeting feature to the exosome surface. Despite this initial success, the restrictive M-shaped topology of full-length CD63 may hinder specific applications that require N- or C-terminal display of cell-targeting moieties on the outer surface of the exosome. In this study, we describe new and topologically distinct CD63 scaffolds that enable robust and flexible surface engineering of the exosome. In particular, we conducted sequential deletions of the transmembrane helix of CD63 to generate a series of CD63 truncates, each genetically-fused to a fluorescent protein. Molecular and cellular characterization studies showed truncates of CD63 harboring the transmembrane helix 3 (TM3) were correctly targeted and anchored to the exosome membrane and exhibited distinct n-, N-, Ω-, or I-shaped membrane topologies in the exosomal membrane. We further established that these truncates retained robust membrane-anchoring and exosome-targeting activities when stably expressed in the HEK293 cells. Moreover, HEK293 cells produced engineered exosomes in similar quantities to cells that expressed full-length CD63. On the basis of the results of our systematic sequential deletion studies, we propose a model to understand molecular mechanisms that underlie membrane-anchoring and exosome targeting features of CD63. In summary, we have established new and topologically distinct scaffolds based on engineering of CD63 that enable flexible engineering of the exosome surface for applications in disease-targeted drug delivery and therapy.

*Corresponding author: blu2@scu.edu and gmlab@berkeley.edu.

Author contributions

B Lu developed the hypothesis, designed experimental approach, performed experiments, analyzed the data, coordinated the project and wrote the manuscript. G Marriott designed experiments, analyzed and interpreted data, revised the manuscript, and added new content and perspectives. N Curley, D Levy, M Do, A Brown, Z Stickney conducted the experiments and aided in preparation of the manuscript.

Competing financial interests

All authors declare no competing financial interests.

Keywords

CD63; exosome; extracellular vesicle; surface display; nanotechnology

INTRODUCTION

Exosomes are an emerging class of biocompatible vehicle for disease-targeted drug delivery and therapy[1-6]. Exosomes originate from special microdomains of the plasma membrane (PM) via poorly understood mechanisms that include two inverted budding processes[7-9]. The primary endocytic event associated with exosome genesis may originate at lipid rafts on the plasma membrane. This budding leads to the formation of the early endosome, which is followed by another inverted budding to produce exosomes and later the multvesicular bodies (MVBs). The second budding involves the loading of bioactive cargo in the lumen of exosomes that include specific cytosolic proteins, mRNAs and microRNA. Exosomes are produced and stored within MVBs prior to their release to the extracellular environment after the fusion of MVGs with the plasma membrane[7-9]. Exosomes offer additional advantages over artificial liposomes, polymer-drug conjugates, and gold/silver particles for therapeutic applications in humans, including high bioavailability, biocompatibility, long circulation times, programmability and the targeted-delivery of large therapeutic payloads[2, 10-16]. Moreover, since exosomes are also produced by diseased cells they can serve for liquid biopsy-based analyses of signature proteins and nucleic acids in the diagnosis of specific diseases, including cancer and neurological diseases and infection[17-22]. The ability of exosomes to shuttle proteins, nucleic acids and lipids between remote cells in the body for applications in drug delivery and therapy has been investigated by many groups[23-27]. For example, El-Andaloussi et al. showed that neurotrophic exosomes can selectively deliver a bioactive siRNA cargo to the brain of a mouse model[28]. Later, Kamerkar et al. showed that surface-modified exosomes loaded with therapeutic siRNAs were more effective than native exosomes in the delivery of their cargo to target cells[3]. In addition to the transport of RNA cargo, we and others have also shown that exosomes can be engineered to deliver protein therapeutics to treat inflammation[6, 29]. Collectively, these proof-of-concept studies demonstrate the feasibility of using exosomes to deliver therapeutic biologics to target cells sites for the treatment of neurological disorders, inflammation and cancer.

As indicated, poor cell-targeting and the absence of therapeutic cargo undermine the usefulness of native exosomes as therapeutic vehicles[10, 30-33]. To overcome these limitations, one needs to identify and incorporate robust biocompatible molecular scaffolds to exosomal membrane to generate gain of function properties, for example by introducing a cell-targeting moiety on the surface and biologics in their lumen. The uptake of these biologics by target cells is designed to trigger their apoptosis, or, in the case of human lysosomal storage diseases, to provide the diseased cell with a functional enzyme[34]. While a number of molecular scaffolds have been studied for these purposes, few generate exosomes that exhibit robust cell-targeting and drug-delivery functions.[28, 30, 35-39].

Here, we introduce a molecular engineering approach to introduce targeting functions to the surface of exosomes produced in human cells. The objectives of this study are: (1) to identify topologically distinctive truncates of CD63 for exosome surface engineering, and (2) to reveal critical domains of CD63 that are responsible for membrane entry and exosome targeting. We realized these objectives using an approach in part by evaluating the effects of sequentially deleting transmembrane domains from both the N- and C-termini of CD63 (appended with fluorescent proteins) on their integration and topology in the exosomal membrane. Live cell fluorescence microscopy was used to investigate the engineered scaffolds for their stability, insertion in the exosome plasma membrane, expression and ability to release the exosomes in large numbers to external environment. The findings of our study support the view that CD63 is a versatile tool to engineer exosomes as biocompatible nano-vehicles for drug delivery and therapy.

2. MATERIALS AND METHODS

2.1 Materials

Transfection reagents Lipofectamine and FuGENE6 were purchased from ThermoFisher Scientific (Waltham, MA) and Promega (Madison, WI) respectively. ExoQuick-TC, Exosome ELISA kit, XPACK-RFP and Dot blot antibody array (antibodies for exosome markers of CD63, CD81, ALIX, Flot1, ICMA1, EpCam, ANXAS and TSG101, as well as a cytosolic protein control GM130) were purchased from System Biosciences (SBI, Palo Alto, CA). Human embryonic kidney cells (HEK293) were purchased from Alstem (Richmond, CA) and human glioblastoma cells (U87) were from the American Type Culture Collection (ATCC, Manassa, VA). Dulbecco's Modified Eagle Medium (DMEM), fetal bovine serum (FBS), and puromycin reagent were purchased from ThermoFisher (Fremont, CA). UltraCULTRE medium was purchased from Lonza (Allgendale, NJ).

2.2 Expression vector construction

The C-terminal fusion expression vector of human tetraspanin CD63 fused to GFP or RFP was constructed as previously reported[35]. Sequential deletion of the transmembrane domain of CD63 was achieved by using a site-directed mutagenesis service from GenScript (Piscataway, NJ). The deletion sites for the removal of transmembrane domains of CD63 were between amino-acids 46-47, 79-80 or 133-134 of CD63 as shown in Figure 1S. The resulting vectors were subjected to double-stranded DNA sequencing to confirm in-frame deletion of the CD63 sequences. The configurations of all constructs used in this study are summarized in Figure 2S.

2.3 Cell culture and transfection

HEK293 and U87 cells were maintained in high glucose DMEM supplemented with 10% FBS, 2 mM and 100 U/mL penicillin and streptomycin at 37°C and 5% CO_2. Transfections were performed in either 3-cm dishes or 6-well plates as previously described[40]. Briefly, cells at 40~60% confluency were transfected with 1~2 μg/well plasmid DNA with either Lipofectamine or FuGENE6 transfection reagents. For transient transfections, cells were incubated with the transfection mix for up to 72 hours resulting in the transfection of over 80% of cells.

2.4 Establishment of stable cell lines

Following their transient transfection for 48 hours, HEK293 cells were switched to a culture medium containing 5 μg/mL puromycin. Stable cell lines were considered to be established if they continued to be GFP/RFP positive and puromycin-resistant for over 8 weeks. The stablely-transfected cells were maintained in the complete selection medium for maintenance but switched to puromycin-free culture condition for at least two passages before conducting any experiments.

2.5 Exosome preparation

Exosomes were prepared from the conditioned medium of stably transfected cells by using a combination of centrifugation, ultrafiltration and chemical precipitation, as previously reported[6]. Typically, cells at 70~80% confluency were switched to serum-free UltraCULTURE to allow for the accumulation of exosomes. After an additional 48 hours, we collected medium from ~$3x10^7$ cells cultured in two 15-cm dishes, followed by centrifugation at 1500xg for 10 min and ultra-filtration through a 0.2 μm syringe filter to remove cell debris and larger particles (typically greater than 200 nm in diameter). The exosomes that remained in the conditioned medium were precipitated by the addition of ExoQuick solution (1:4 dilution) and centrifuged at 3,000xg for 90 min at 4°C. The pelleted exosomes were resuspended in PBS and stored at −80°C for future use. We have submitted all relevant data of our experiments to the EV-TRACK knowledgebase (EV-TRACK ID: EV2000210) with an EV-METRIC score of 44%[41].

2.6 Dot-blot immune-assay of exosome markers

Exosomes isolated from conditioned medium were analyzed for exosome-biomarkers using a premade membrane blot as previously described[29]. Each blot featured 8 antibodies against exosome markers (CD63, CD81, ALIX, Flot1, ICMA1, EpCam, ANXAS and TSG101, as well as a cytosolic protein control GM130)[42]. The dot-blot assays were performed using a service provided by SBI (Palo Alto, California).

2.7 Nanoparticle tracking analysis (NTA)

The particle concentration, size-distribution of the isolated exosomes were analyzed by a NonoSight LM10 instrument (Malvern Instruments Ltd, Malvern, UK) as previously reported[6]. In a typical analysis, 1 mL of a 1:1000 time-diluted exosome sample was prepared for particle visualization and recording of light scattering. Three videos, each of 60 seconds recordings, were analyzed and results were plotted to show particle concentration, size and distribution.

2.8 Fluorescence and confocal microscopy

Live cell imaging was conducted using either an Olympus fluorescence microscope (Waltham, MA) or a Zeiss LSM700 confocal microscope (Carl Zeiss Vision Inc. San Diego, CA). Both fluorescence and light transmitted images were recorded at indicated time-points to reveal the intracellular localizations of exosome-labeled fluorescent fusion proteins. In the case of the confocal fluorescence data, we recorded optical image slices of the sample

recorded at a vertical depths and used Image J software. Adjustments to the brightness and contrast of images were made for the entire z-frame.

3. RESULTS AND DISCUSSION

3.1 Design and construction of topologically-distinct CD63 truncates

We and others had previously shown that full-length human CD63 first integrates into the ER lipid bilayer and is then quickly funneled to the plasma membrane where it localizes to lipid microdomains known as tetraspanin-enriched microdomains (TEMs)[43, 44]. As a key molecular organizer, CD63 recruits other lipid raft proteins to TEMs and serves as an initiation site for the formation of both endosomes, and later exosomes via two consecutive inverted membrane budding processes (Figure 1A). Lacking a signal peptide, CD63 may participate in the ER membrane via one of its transmembrane domains in a similar manner as other seven-transmembrane proteins[45-48]. Accordingly, we elected to use a sequential deletion strategy to create a set of CD63-truncates to determine which, if any, transmembrane domain is necessary for the localization of CD63 to the exosome surface. By progressive deletion of the transmembrane domains from either N- or C-terminus of CD63, we generated a new set of CD63-truncates that show distinct membrane topologies, including the original M-shape of full-length CD63 (Figure 1A). Specifically, the N-terminal deletions create n-, Ω-, or I-shape truncates, predicted from the established M-shape membrane topology of full-length CD63 (Figure 1B, **upper panels**). Likewise, C-terminal deletions produce N-, Ω-, or I-shape truncates (Figure 1B, **middle panels**). Simultaneous deletions from both N- and C-terminus generates the transmembrane domain-3 (CD63TM3), which also has an I-shape geometry (Figure 1B, **bottom panel**), and is similar to those present in CD63TM1 and CD63TM4. After establishing protocols to generate this new set of CD63 truncates, we conducted further engineering steps to produce a cohort of molecular scaffolds of unique geometry for exosome engineering. In particular, these CD63 truncates enable a flexible and programmable approach to display polypeptide-based targeting moieties and sensor probes on the outer surface of the exosome, while loading the inner lumen with protein-based therapeutics as depicted in Figure 1A (**Lower panel, EXOSOME**). Figure 1C summarizes the identifiers and topologies of these engineered proteins, including full-length wild-type CD63 and eight truncated variants of CD63.

Next, we used this design strategy to generate a family of 12 vectors for experimental studies, including 3 full-length CD63 and 8 CD63-truncates (Figure S2). To allow for live cell imaging of the molecular movements and abundances of CD63 and its truncates, we tagged the proteins with either fluorescent proteins and/or puromycin-resistant proteins at the C-terminus (Figure S2). These CD63 fusions enabled us to (1) monitor and identify critical domains for both membrane-anchoring and exosome-targeting; (2) validate whether those CD63 truncates can serve as potential molecular scaffolds for protein loading or surface display; (3) to establish stable cell lines to test the robustness of these CD63-based scaffolds for long-term imaging and tracking.

3.2 Configuration of CD63 from M-shape to n- or N-shape

It is well known that the human full-length CD63 exhibits an M-shape topology on the plasma membrane[44, 47]. In this setting, four transmembrane domains of CD63 are embedded in phospholipid bilayer, two exist as extracellular loops on the outer surface, while the middle loop, and the N- and C-termini of the fusion protein are positioned on the inner surface of the exosome membrane, *i.e.*, an M-shaped membrane topology (Figure 1A). This configuration of the full-length CD63 restricts the location of the N- and C-termini to the lumen of the exosome, which limits applications of engineered exosomes, for example in displaying cell-targeting proteins on the outer surface. We note that with the removal of the first transmembrane domain, the shortened CD63 would lose its N-terminus within the lumen but gain a new N-terminus on the outer surface of the exosome membrane, *i.e.*, an "n"-shaped membrane topography. Similarly, deletion of the C-terminus will generate a new C-terminus exposed to the outside surface of the exosome membrane. These CD63-truncates are significant and highly-valued, in part because they allow for programmable control of targeting moieties at both termini, for example to display a capture group on the external face of the exosome membrane and a protein-therapeutic on the inner (lumen) face of the membrane for applications in targeted-delivery of biologics to diseased tissue.

First, we focused our attention on the generation and properties of the n- and N-shaped membrane topographies, namely CD63n (N-terminal TM1 truncate) and CD63N (C-terminal TM4 truncate). We examined whether CD63n retained its abilities to integrate correctly in the exosome membrane and to function as an exosome-targeting group. We used exosomes harboring full-length CD63M as a reference for these studies. To this end, we transfected HEK293 cells with CD63n-GFP alone and monitored its expression and subcellular distribution using fluorescence microscopy. Images of cells expressing CD63n-GFP-Puro were characterized by numerous green fluorescent puncta in the cytosol (Figure 2A-C), consistent with our previously reported images of GFP fusions with CD63M[35]. To confirm that CD63n integrates into the same membranes as full-length CD63, we co-transfected HEK293 cells with both CD63n-GFP-Puro and CD63M-RFP. Fluorescence images of both cells expressing both CD63n-GFP-Puro and CD63M-RFP exhibited a significant degree of overlap in the distributions of fluorescent puncta, suggesting they are integrated into the same membranes (Figure 2D-F). These results indicate that CD63n is capable of integrating in correct membrane compartments during exosome biogenesis.

Next, we used the same approach to determine if CD63N can also localize and integrate into exosomes. Similar to CD63n, we found the fluorescence images of cells expressing the CD63N-RFP construct were characterized by numerous cytosolic puncta, consistent with previously reported images of GFP fusions with CD63M[6] (Figure 2G-H). Fluorescence images of cells co-transfected with full-length CD63M-GFP and CD63N-RFP were found to exhibit identical, overlapping fluorescence signals (Figure 2J-K), suggesting they integrate into the same membrane compartments. Taken together, our results show that the N-terminal TM1 truncate (CD63n) and the C-terminal TM4 truncate (CD63N) are correctly integrated and functional in the exosome membrane. These studies also showed that TM1 and TM4 transmembrane domains of CD63 are not necessary for exosome targeting.

Next, we asked if the CD63 fusion proteins including the M-, n-, and N-shaped CD63 (CD63M, CD63n and CD63N), are localized exclusively to exosomes during their biogenesis in the cytosol. First, we recorded high-resolution confocal fluorescence microscopy images of each fusion protein in cells to show they were confined to the cytosol. In brief, after transfection of cells with either of CD63n-GFP-Puro, or CD63N-RFP, or CD63M-GFP-Puro for 48 hours, we labeled the cells with Hoechst dye to highlight their nuclei (blue). Fluorescence and light transmitted images of the blue, green and red-emitting cells were recorded at defined z-sections of the sample using the confocal microscope. Overlay images of the CD63n-GFP-Puro and CD63N-RFP fluorescence revealed identical punctate staining in the cytosol. Identical staining was also found in cells co-expressing CD63M-GFP-Puro (Figure 3A-B, **green**) and CD63N-RFP (Figure 3C-D, **red**) (Figure 3E-F, **green**). We confirmed these CD63 variants localize to cytosol compartments in additional studies using human HepG2 cell lines (Supplementary Figure S4). Next, we showed the fusion proteins were exclusively localized to exosomes using a co-transfection image analysis approach that included co-expression of the exosome marker, XPACK. We labeled XPACK with either RFP (for co-transfection with CD63n-GFP-Puro) or GFP (for co-transfection with CD63N-RFP). We recorded the expression of each protein at 48-hours post-transfected using confocal fluorescence microscopy. As shown in Figure 3G-J, we found significant overlap of the two fluorescent signals originating from the TM1-deleted truncate CD63n-GFP-Puro and XPACK-RFP (Figure 3J, **yellow, arrow**). Similar labeling patterns were recorded for the TM4-deleted truncate CD63N-RFP (Figure 3K-N), a finding that also suggested the fusion protein colocalized with XPACK-GFP (Figure 3M, **yellow, arrow**). As expected, we found the expression patterns of each fusion protein and XPACK were similar to that of full-length CD63M-GFP-Puro (Figure 3O-R). Taken together, our results demonstrate that the deletion of either the first (TM1) or the last (TM4) transmembrane domain of CD63 does not alter the ability of each truncate to integrate in the exosome membrane, *i.e.*, TM1 and TM4 are not required for correct exosome targeting and participation.

3.3 *Configuration of CD63 from M- to Ω-shape*

Next, we determined which of the domains of CD63 are required for exosome targeting by introducing progressive deletions from each end of full-length CD63. We also investigated the effects of specific deletions on the locations of the N- and C-termini, ie, projecting to the external surface or to the lumen. In particular, we constructed the following truncated forms of CD63: CD63ΩTM1-2 (deletion of TM3 and TM4) and CD63ΩTM3-4 (deletion of TM1 and TM2). We predicted both truncates would have a Ω-shape topology with both termini situated inside the lumen, *i.e.,* similar to full-length CD63. To examine how the two truncates are arranged in the exosome membrane, we added a GFP gene to each truncate followed by transfection in HEK293 cells. Finally, we imaged the GFP-fluorescence emission of the transfected cells. In the case of cells transfected with only CD63ΩTM1-2-GFP or CD63ΩTM3-4-GFP-Puro, we found the green fluorescence localized to punctate structures in the cytosol, which suggest they integrated in intracellular endosomes (Figure 4A-C, J-L). To confirm this result, we co-transfected these cells with full length CD63M-RFP. In another study, we co-transfected cells with CD63ΩTM3-4-GFP-Puro and the exosome marker XPACK-RFP. Analysis of the fluorescence images of these cells revealed

signals arising from CD63ΩTM3-4-GFP-Puro with full length CD63M-RFP (Figure 4D-F) and CD63ΩTM3-4-GFP-Puro with the exosome marker XPACK-RFP (Figure 4G-I), as evidenced by the strong yellow color in the overlay images for both exosome markers (Figure 4F and 4I). These results indicate that CD63ΩTM3-4-GFP-Puro is correctly targeted to and integrated in the exosomal membrane. In contrast, the corresponding overlap image of cells co-transfected with CD63ΩTM1-2-GFP and either full-length CD63M-RFP (Figure 4 M-O), or RFP-XPACK (Figure 4 P-R) did not show co-localization of the fluorescence signals. Thus, CD63 ΩTM1-2 is not directed to exosomes but rather to some other compartment. Since CD63ΩTM3-4 (TM1 and TM2 deletion) correctly integrates into exosomes, and because CD63ΩTM1-2 (TM3 and TM4 deletion) loses its ability to integrate into exosomes, we conclude that TM3 and/or TM4 are critical for correct localization of CD63 to the surface of the exosome.

3.4 TM3 alone is both required and sufficient for correct exosome targeting and anchoring

Having shown TM3 and/or TM4 are essential for correct targeting and anchoring of CD63 truncates to exosomes, we tested the hypothesis that TM3 alone is sufficient for the correct integration of CD63 into exosomes. To this end, we created CD63 truncates harboring a single transmembrane domain truncate, namely GFP fusions of CD63ITM3 (TM3-only), CD63ITM1 (TM1-only) and CD63ITM4 (TM4-only). In some studies, the cells were also transfected with full length CD63. After 48-hours (post-transfection), we recorded fluorescence images of cells expressing one of the I-shaped truncates alone, or in some cases in cells co-transfection with full length CD63 (Figure 5). As expected, both CD63ITM1-GFP (Figure 5 A-C) and CD63ITM4-GFP (Figure 5 G-I) showed a uniform distribution of fluorescence in the cytosol (Figure 5 B-C, H-I), which suggested they do not integrate in intracellular vesicles. In contrast, fluorescence images of cells expressing CD63ITM3-RFP alone were characterized by a punctate staining of their cytosol (Figure 5 C-F). We confirmed these puncta originated from exosomes by recording and analyzing fluorescence images of CD63ITM3-RFP and CD63M-GFP in co-transfected cells - the overlayed fluorescence image showed cytosolic puncta were co-labeled with the two fusion proteins (Figure 5 M-O). On the basis of this study we conclude that the TM3 domain alone is sufficient and necessary for CD63 localization to the exosome surface. As expected from our earlier study, the fluorescence overlap images of cells co-transfected with CD63M-GFP and CD63ITM1-GFP (TM1-only), or CD63M-GFP and CD63ITM4-GFP (TM4-only) showed little correlation between the two fluorescence signals (Figure 5 J-H, P-R). These results are in line with the conclusion of our earlier study that TM3 but not TM1 or TM4 are sufficient and necessary for correct exosomal targeting.

To confirm the generality of this conclusion, we conducted co-transfection studies using a human glioblastoma cell line. U87 cells were co-transfected with CD63ITM3-RFP (TM3-only) and either full-length CD63M-GFP, or the exosome marker XPACK-GFP. After 3-days we recorded fluorescence images in the GFP and RFP channels. As shown in the Supplementary Figure S3, the images of cells transfected with CD63ITM3 (Figure S3 A1, B1) revealed a punctate distribution of red fluorescence in the cytosol that correlated with signals from CD63M-GFP (Figure S3 A2-3), and XPACK-GFP (Figure S3 B2-3). We

conclude from this study that the TM3 domain is sufficient and necessary for exosome targeting to U87 cells.

Our finding that the TM3-domain is both necessary and sufficient for correct exosome targeting and anchoring in diverse human cell types represents an important breakthrough in our understanding of the molecular mechanism that underlies the targeting and integration of CD63 in exosomal membranes. Also significant, is the identification of TM3 as a new topological distinct scaffold for surface engineering of exosomes for applications in nanomedicine.

3.5 Novel CD63 scaffolds enable robust and versatile surface engineering of exosome

We created a cohort of CD63 truncates through sequential deletion of the full-length gene – each truncate displays a distinct membrane topology that differs from full-length CD63. In particular, we draw attention to the TM3-containing truncates CD63n, CD63N and CD63ITM3 (TM3 only) that display their N- or C-terminus on either the outer surface of the exosome or in the exosome lumen. This feature is highly-valued in exosome engineering – for example, by appending proteins to each terminus, one can simultaneously generate exosomes that are capable of binding to a receptor target on a diseased cell and on internalization load therapeutic proteins in the lumen to the targeted cell. One the basis of our earlier studies, we selected two truncates (CD63n and CD63N) for further exosome engineering and compared their physical and functional properties to exosomes engineered with full length CD63. We established the following goals for these studies: (1) to permanently express chimeric protein in human producer cells; (2) to develop human cell systems for robust production of engineered exosomes using these producer cells; and (3) to optimize the secret genetically modified exosomes to the extracellular environment.

First, we investigated the ability of cells to support the permanent expression and integration of CD63n-GFP-Puro, CD63N-RFP and CD63M-GFP-Puro in exosomes. After transfecting cells, puromycin was added to the culture medium at 48-hours to initiate a 20-round selection process to isolate populations of transformed cells that permanently express the fusion protein in exosomes (Figure 6A). We used fluorescence microscopy to monitor the expression of CD63 fusions over 20 cell passages. These studies identified punctate fluorescent staining of the cytosol in both the CD63n-GFP-Puro (Figure 6B-D) and the CD63N-RFP (Figure 6E-G) transfected cells. The labeling was similar to that reported which are comparable to those of CD63M-GFP-Puro (Figure 6H-J), which suggests the two truncates are, like full length CD63, suitable for long-term production of genetically-engineered exosomes.

Next, we examined the release of these genetically modified exosomes from the cytosol of source cells to the external environment. We used transformed cells that expressed either CD63n-GFP, CD63N-RFP or CD63M-GFP. First, we isolated the exosomes from the conditioned medium of each transformed cell type and then recorded high resolution fluorescence images of each exosome preparation. As shown in Figure 7A, exosomes containing CD63n-GFP-Puromycin (Figure 7A-2, **green**) or CD63N-RFP (Figure 7A-4, **red**) emitted a strong fluorescence similar to that described for CD63M-GFP-Puro containing exosomes (Figure 7A-1, **green**). On the other hand, we did not detect fluorescent

signals in exosomes from control (un-modified) cells (Figure 7A-3, 5). Please note that green/red fluorescence may represent individual particles or their aggregates, which do not correlate to their sizes due to the spatial resolution limit of the light microscopy (~225 nm). Given the weaker fluorescence signals of RFP compared to GFP, the fluorescent intensity recorded in different exosome smears may not correlate with the efficacy of labeling. On the basis of this study, we conclude CD63-truncate-engineered exosomes, like those harboring full length CD63, are released from their mother cell to the extracellular environment. To determine whether those genetic modifications alter the quantity of exosomal production, we used an ELISA-kit to quantify marker proteins on the purified exosome preparations produced by each cell type. We did not find any meaningful difference in the quantity of exosomes released from number-normalized producer cells that expressed exosomes containing CD63M-GFP-Puro, CD63n-GFP-Puro or CD63N-RFP, or the number produced in the non-modified control (Figure 7B). A closer analysis of the exosomes using a laser-based nano-particle tracking system showed most particles had a diameter within the range of 90~130 nm (Figure 7C). Moreover, we did not find any significant differences in the distribution of particle size among engineered exosomes containing either truncated forms of CD63, full length CD3 or unmodified exosomes from the control cells (Figure 7C). Finally, we conducted an immuno-blot analysis to identify multiple exosome-specific protein markers on the engineered and control exosomes. We found all exosome types tested positive for the biomarker proteins, including Flot1, ICAM, CD81, CD63, ANX5, TSG101, but not for the cytosolic protein, GM130. We conclude our physical and molecular characterization of engineered and control exosomes that those expressing CD63n and CD63N derived from human producer cells are authentic, free of cytosolic contaminants (Figure 7D), stable and produced over an extended period from transformed human cells in quantities that make them attractive as novel therapeutic agents for basic research and clinical translation. Importantly, these modified exosomes appear to retain their ability to enter human cells, including human kidney (HEK293) and human hepatic (HepG2) cells (Supplementary Figure S5), indicating a functional preservation if used as delivery tools.

3.6 Molecular model for exosome targeting and anchoring of CD63

Although the integral membrane protein CD63 is known to be highly enriched on exosomes, we know little of how it is recruited and integrated in the ER membrane and subsequently to the exosomal membrane. Our studies have shed some light on this mechanism. In particular, our sequential domain deletion has identified the TM3 being necessary and sufficient for membrane anchoring and exosome targeting (Figure 8A). In our model of CD63 function, TM3 is proposed to act as a start-transfer signal and that initiates the transfer of hydrophobic α-helices across the bilayer of the ER membrane. Once anchored, the insertion of the membrane-spanning helices of TM4 establishes the final topology of the C-terminus. Similarly, TM2 acts as the second start-transfer signal that directs the growing polypeptide chain (to the N-terminus) to the lumen. In this way, CD63 integrated in the ER membrane with an M-shaped topology. This topology dictates the orientation of CD63 in all subsequent membranes, including the plasma membrane, endosomes and exosomes. Because CD63 is always synthesized within the cytosol, all copies of CD63 will have the same membrane topology that is preserved during the membrane fusion and budding events that eventually lead to its integration in exosomes. The fact that all of TM3 containing truncates we

investigated, including CD63n, CD63N and CD63-TM3-only are faithfully integrated and targeted to the exosome with the same topology as the full length CD63 may suggest TM3 harbors multi-molecular signaling motifs. Although TM2-containing variants are also able to integrate into membranes of intracellular vesicles, their distribution in human cells differs from those of the full-length CD63, most likely due to the absence of an exosome-specific signal.

The findings of our study are significant on several counts: First, we engineered exosomes in human cell lines that stably express TM3-containing fusion proteins that are correctly directed and integrated into the exosomal membrane. Second, the engineered exosomes are secreted in large numbers from diverse human cells and are easily isolated from the conditioned medium using standard practices. Third, exosomes released from cells that stably-express CD63 truncates are indistinguishable in their size distribution and protein biomarker content from those produced in un-modified cells. Fourth, by using different configurations of TM3 in unions with other domains of CD63, we can robustly control the topology of one or more functional proteins fused to the N- and C-termini of the CD63-truncate. This property allowed us to project disease-targeting proteins to the external face of the exosomal membrane, and to direct a protein-based therapeutic to the lumen. The study highlights a path to engineer exosomes for applications in the diagnosis and treatment of human diseases. For example, one could isolate exosomes from conditioned medium that express a CD3 truncate (TM3 and TM4) whose C-terminus is fused to an engineered antibody directed against a tumor cell biomarker, and whose N-terminus is fused to a protein that on uptake by the target cell induces apoptosis.

3.7 Current status and future development

Recently, Gau X and colleagues have demonstrated that a peptide identified by phage display enables direct modification by specific binding and cargo loading to the second extracellular loop CD63[49]. This method may provide a simple means of cargo loading but restrict cargo loading to the outer surface of exosome, which may be subject to degradation in circulation. Using a light-inducible module, Yim N and colleagues have been able to attach soluble proteins to the C-terminus of CD9 [29]. This method, however, limits the cargo loading to the lumen. We have shown that our genetic method provides a stable method for cargo loading via gene fusion, which is not possible using the peptide-modification. Importantly, our new CD63 scaffolds enable more sophisticated engineering and provide greater flexibility in presenting bioactive cargos in a desirable geometrical and sterical manner.

The use of CD63 variants for both exosome targeting and drug loading is intriguing and if successful would represent a major advance in the field. For example, CD63n allows one to display of targeting moieties, such as signal-chain variable fragment, on the outer surface, and to simultaneously load therapeutic proteins, such as beta glucocerebrosidase, inside lumen of exosomes (A. Brown - unpublished observations). Future studies are planned to investigate the potential of this strategy in clinical studies.

Supplementary Material

Refer to Web version on PubMed Central for supplementary material.

Acknowledgments

We thank Grace Ling, Hanzhe Chen, David Diebold and Dr. Shu Kan for providing excellent assistance in taking and processing confocal and fluorescent images. We also thank Dr. Yan Jiang for her careful reading and revision of the manuscript. Professor Marriott acknowledges support from the Tsinghau-Berkeley Shenzhen Institute. This work was supported by funds from the School of Engineering at Santa Clara University and by the National Institute of General Medical Sciences of the National Institutes of Health under Award Number R15GM137449. The content is solely the responsibility of the authors and does not necessarily represent the official views of the National Institutes of Health.

Abbreviations

CMV	cytomegalovirus promoter
FBS	fetal bovine serum
GFP	green fluorescent protein
RFP	Red fluorescent protein
MVB	multi-vesicular body
TM	transmembrane domain

REFERENCES

1. Conlan RS, Pisano S, Oliveira MI, Ferrari M & Mendes Pinto I Exosomes as Reconfigurable Therapeutic Systems. Trends Mol Med 23, 636–650. [PubMed: 28648185]
2. Gyorgy B, Hung ME, Breakefield XO & Leonard JN Therapeutic applications of extracellular vesicles: clinical promise and open questions. Annu Rev Pharmacol Toxicol 55, 439–464. [PubMed: 25292428]
3. Kamerkar S et al. Exosomes facilitate therapeutic targeting of oncogenic KRAS in pancreatic cancer. Nature 546, 498–503 (2017). [PubMed: 28607485]
4. Marcus ME & Leonard JN FedExosomes: Engineering Therapeutic Biological Nanoparticles that Truly Deliver. Pharmaceuticals (Basel) 6, 659–680 (2013). [PubMed: 23894228]
5. Vader P, Mol EA, Pasterkamp G & Schiffelers RM Extracellular vesicles for drug delivery. Adv Drug Deliv Rev 106, 148–156. [PubMed: 26928656]
6. Duong N et al. Decoy exosomes as a novel biologic reagent to antagonize inflammation. Int J Nanomedicine 14, 3413–3425. [PubMed: 31190800]
7. Kowal J, Tkach M & Thery C Biogenesis and secretion of exosomes. Curr Opin Cell Biol 29, 116–125 (2014). [PubMed: 24959705]
8. Colombo M, Raposo G & Thery C Biogenesis, secretion, and intercellular interactions of exosomes and other extracellular vesicles. Annu Rev Cell Dev Biol 30, 255–289 (2014). [PubMed: 25288114]
9. Mittelbrunn M & Sanchez-Madrid F Intercellular communication: diverse structures for exchange of genetic information. Nat Rev Mol Cell Biol 13, 328–335 (2012). [PubMed: 22510790]
10. Vlassov AV, Magdaleno S, Setterquist R & Conrad R Exosomes: Current knowledge of their composition, biological functions, and diagnostic and therapeutic potentials. Biochimica et Biophysica Acta (BBA) - General Subjects 1820, 940–948 (2012). [PubMed: 22503788]
11. Valadi H et al. Exosome-mediated transfer of mRNAs and microRNAs is a novel mechanism of genetic exchange between cells. Nat Cell Biol 9, 654–659 (2007). [PubMed: 17486113]

12. Simpson RJ, Jensen SS & Lim JW Proteomic profiling of exosomes: current perspectives. Proteomics 8, 4083–4099 (2008). [PubMed: 18780348]
13. Thery C Exosomes: secreted vesicles and intercellular communications. F1000 Biol Rep 3, 15.
14. Antes TJ et al. Targeting extracellular vesicles to injured tissue using membrane cloaking and surface display. J Nanobiotechnology 16, 61. [PubMed: 30165851]
15. Ha D, Yang N & Nadithe V Exosomes as therapeutic drug carriers and delivery vehicles across biological membranes: current perspectives and future challenges. Acta Pharm Sin B 6, 287–296. [PubMed: 27471669]
16. Kim BY, Rutka JT & Chan WC Nanomedicine. N Engl J Med 363, 2434–2443.
17. Lin J et al. Exosomes: novel biomarkers for clinical diagnosis. ScientificWorldJournal 2015, 657086. [PubMed: 25695100]
18. Melo SA et al. Glypican-1 identifies cancer exosomes and detects early pancreatic cancer. Nature 523, 177–182. [PubMed: 26106858]
19. Pulliam L, Sun B, Mustapic M, Chawla S & Kapogiannis D Plasma neuronal exosomes serve as biomarkers of cognitive impairment in HIV infection and Alzheimer's disease. J Neurovirol.
20. Soung YH, Ford S, Zhang V & Chung J Exosomes in Cancer Diagnostics. Cancers (Basel) 9.
21. Peinado H et al. Melanoma exosomes educate bone marrow progenitor cells toward a pro-metastatic phenotype through MET. Nat Med 18, 883–891. [PubMed: 22635005]
22. Jalalian SH, Ramezani M, Jalalian SA, Abnous K & Taghdisi SM Exosomes, new biomarkers in early cancer detection. Anal Biochem 571, 1–13. [PubMed: 30776327]
23. Shahabipour F, Banach M & Sahebkar A Exosomes as nanocarriers for siRNA delivery: paradigms and challenges. Arch Med Sci 12, 1324–1326.
24. Sterzenbach U et al. Engineered Exosomes as Vehicles for Biologically Active Proteins. Mol Ther 25, 1269–1278.
25. Shah R, Patel T & Freedman JE Circulating Extracellular Vesicles in Human Disease. N Engl J Med 379, 958–966. [PubMed: 30184457]
26. Ingato D, Lee JU, Sim SJ & Kwon YJ Good things come in small packages: Overcoming challenges to harness extracellular vesicles for therapeutic delivery. J Control Release 241, 174–185. [PubMed: 27667180]
27. S ELA, Mager I, Breakefield XO & Wood MJ Extracellular vesicles: biology and emerging therapeutic opportunities. Nat Rev Drug Discov 12, 347–357. [PubMed: 23584393]
28. El-Andaloussi S et al. Exosome-mediated delivery of siRNA in vitro and in vivo. Nat Protoc 7, 2112–2126 (2012). [PubMed: 23154783]
29. Yim N et al. Exosome engineering for efficient intracellular delivery of soluble proteins using optically reversible protein-protein interaction module. Nat Commun 7, 12277 (2016). [PubMed: 27447450]
30. Hung ME & Leonard JN Stabilization of exosome-targeting peptides via engineered glycosylation. J Biol Chem 290, 8166–8172. [PubMed: 25657008]
31. Yanez-Mo M et al. Biological properties of extracellular vesicles and their physiological functions. J Extracell Vesicles 4, 27066.
32. Petros RA & DeSimone JM Strategies in the design of nanoparticles for therapeutic applications. Nat Rev Drug Discov 9, 615–627. [PubMed: 20616808]
33. Van Deun J et al. The impact of disparate isolation methods for extracellular vesicles on downstream RNA profiling. J Extracell Vesicles 3.
34. Do MA, Levy D, Brown A, Marriott G & Lu B Targeted delivery of lysosomal enzymes to the endocytic compartment in human cells using engineered extracellular vesicles. Scientific Reports 9, 17274.
35. Stickney Z, Losacco J, McDevitt S, Zhang Z & Lu B Development of exosome surface display technology in living human cells. Biochem Biophys Res Commun 472, 53–59 (2016). [PubMed: 26902116]
36. Shi J, Heegaard CW, Rasmussen JT & Gilbert GE Lactadherin binds selectively to membranes containing phosphatidyl-L-serine and increased curvature. Biochim Biophys Acta 1667, 82–90 (2004). [PubMed: 15533308]

37. Veron P, Segura E, Sugano G, Amigorena S & Thery C Accumulation of MFG-E8/lactadherin on exosomes from immature dendritic cells. Blood Cells Mol Dis 35, 81–88 (2005). [PubMed: 15982908]

38. Shen B, Wu N, Yang JM & Gould SJ Protein targeting to exosomes/microvesicles by plasma membrane anchors. J Biol Chem 286, 14383–14395 (2011). [PubMed: 21300796]

39. Delcayre A et al. Exosome Display technology: applications to the development of new diagnostics and therapeutics. Blood Cells Mol Dis 35, 158–168 (2005). [PubMed: 16087368]

40. Meyer C et al. Pseudotyping exosomes for enhanced protein delivery in mammalian cells. Int J Nanomedicine 12, 3153–3170 (2017). [PubMed: 28458537]

41. Van Deun J et al. EV-TRACK: transparent reporting and centralizing knowledge in extracellular vesicle research. Nat Methods 14, 228–232. [PubMed: 28245209]

42. Kowal J et al. Proteomic comparison defines novel markers to characterize heterogeneous populations of extracellular vesicle subtypes. Proc Natl Acad Sci U S A 113, E968–977. [PubMed: 26858453]

43. Hemler ME Tetraspanin proteins mediate cellular penetration, invasion, and fusion events and define a novel type of membrane microdomain. Annu Rev Cell Dev Biol 19, 397–422 (2003). [PubMed: 14570575]

44. Hemler ME Tetraspanin functions and associated microdomains. Nat Rev Mol Cell Biol 6, 801–811 (2005). [PubMed: 16314869]

45. Fry MY & Clemons WM Jr. Complexity in targeting membrane proteins. Science 359, 390–391. [PubMed: 29371455]

46. Shao S & Hegde RS A flip turn for membrane protein insertion. Cell 146, 13–15. [PubMed: 21729778]

47. Hassuna N, Monk PN, Moseley GW & Partridge LJ Strategies for targeting tetraspanin proteins: potential therapeutic applications in microbial infections. BioDrugs 23, 341–359 (2009). [PubMed: 19894777]

48. Hemler ME Targeting of tetraspanin proteins--potential benefits and strategies. Nat Rev Drug Discov 7, 747–758 (2008). [PubMed: 18758472]

49. Gao X et al. Anchor peptide captures, targets, and loads exosomes of diverse origins for diagnostics and therapy. Sci Transl Med 10.

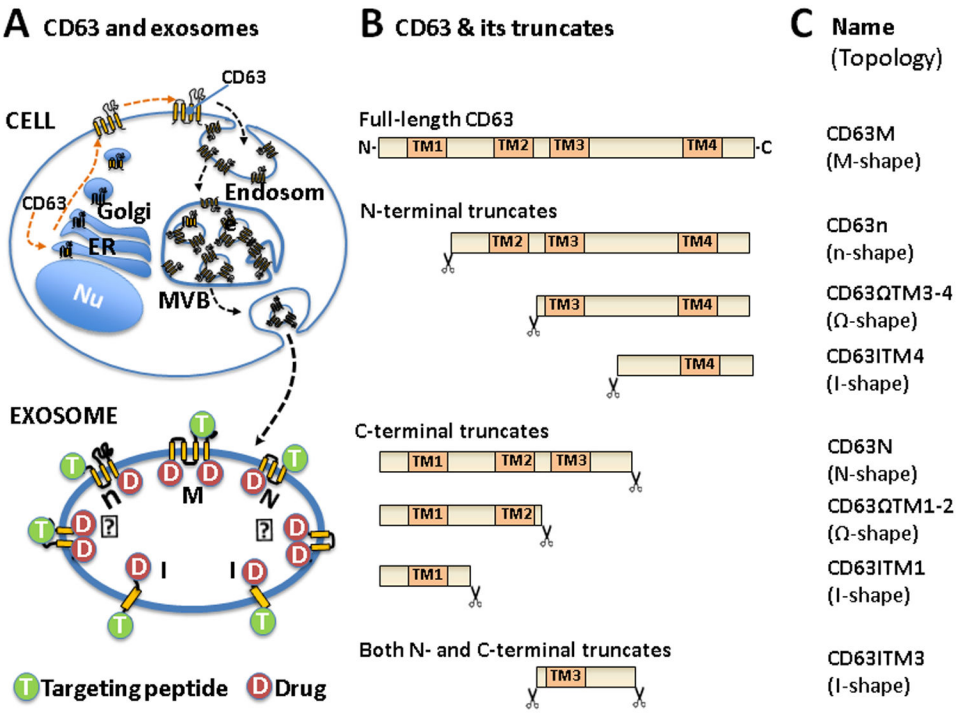

Figure 1. Exosome biogenesis and reconfiguring strategy of CD63 for surface display.

(A top) Cell: the fate of CD63 illustrates both the earlier distribution to the plasma membrane and the later participation into exosomes via two distinctive pathways: 1) the secretory pathway from ER → Golgi → PM (brown dashed lines) and 2) the endocytic pathway from PM endosome MVB → (black dashed lines). Exosome: membrane topology of the full-length or its domain-deleted truncates. Tagged peptides as targeting moiety (T) or protein drug (D) are indicated. (**B**) Exosome: Schematic representation of experimental design and deletion strategy of CD63. The cutting sites are indicated by a scissor sign. (**C**) Names of the full-length CD63 and its truncates as well as their corresponding membrane topology. Circled T (green): targeting peptide on the outer surface of exosome. Circled D (red): protein drugs on the inner surface of exosome.

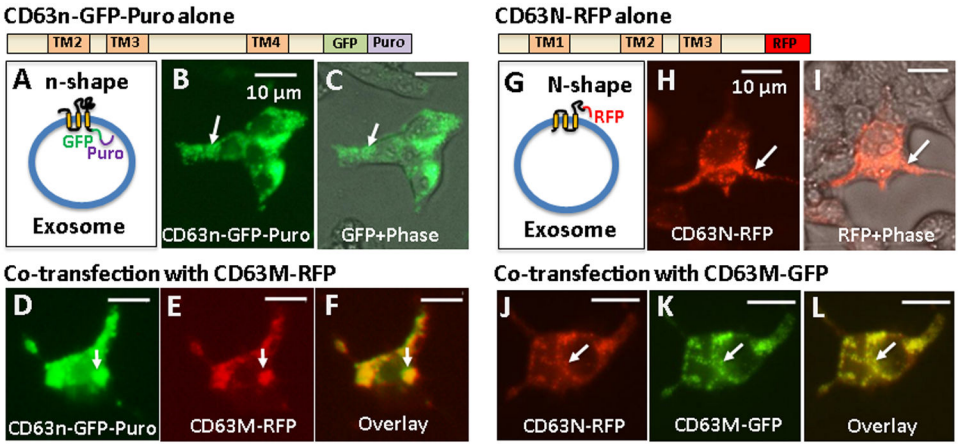

Figure 2. Single TM-deleted truncates (CD63n and CD63N) and their subcellular localization in living HEK293 cells.

Cells are transfected with fusion proteins of either TM1-deleted CD63n-GFP-Puro alone or with the full-length CD63M-RFP (**Left panels, A-F**). At 72 hrs, the CD63n-GFP-RFP alone (**A**) exhibits punctuated GFP fluorescence in the cytosol (**B-C**), where it localizes with the full-length CD63M-RFP as indicated by overlapping of yellow signal (**F, arrow**). In a separate set of experiments, cells were transfected with either TM4-deleted CD63N-RFP alone or with the full-length CD63M-GFP (**Right panels, G-L**). At 72 hrs, the CD63N-RFP (**G**) demonstrated the same intracellular pattern with red fluorescence signals in the cytosol (**H-I**) and co-localization with the full-length CD63M-GFP as shown by overlapping of the yellow signals (**L, arrow**) in transfected HEK293 cells (**J-L**). Arrows indicated endosome/exosome/MVB structures. Scale bar: 10 µm.

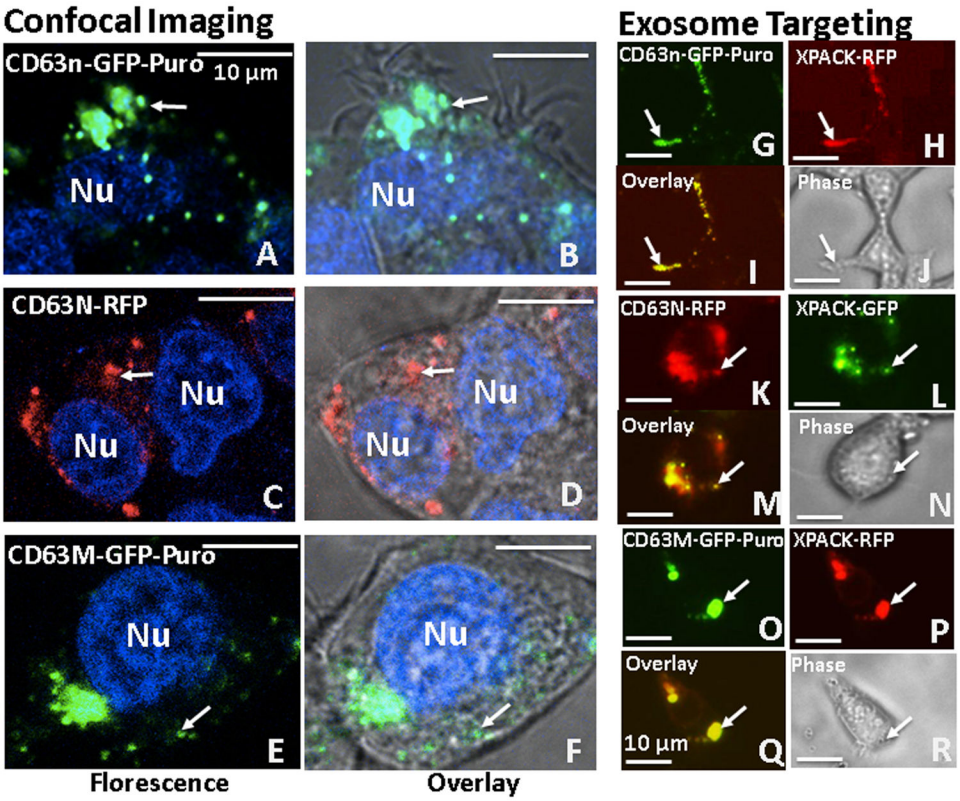

Figure 3. Subcellular localization of the single TM-deleted CD63 truncates (CD63n and CD63N) and their colocalization with either the full-length CD63M or the exosome marker XPACK in living HEK293 cells.

Cells transfected with either CD63n-GFP-Puro, or CD63N-RFP, or CD63M-GFP-Puro for 48 h were strained with Hoechst (blue) and subjected to confocal imaging. Overlaid fluorescent and bright light images show punctuated fluorescent signals localized in the cytosol for both CD63n-GFP-Puro (**A-B, green**) and CD63N-RFP (**C-D, red**), similar to those of the full-length CD63M-GFP-Puro (**E-F, green**). In a separate set of experiments, cells were co-transfected with CD63n-GFP-Puro and the exosome marker, XPACK-RFP (**G-J**); at 48 hr, fluoresce images show that overlapping yellow signal (I, arrow) in the cytosol, suggesting exosomal localization of CD63n. Similar results were obtained when cells were co-transfected with CD63N-RFP and XPACK-GFP (**K-N**), which are consistent with those of the full-length CD63M-GFP-Puro (**O-R**). Arrows indicate the subcellular localization of individual fluorescent protein-fused CD63 or XPACK and their co-localization. Scale bar: 10 μm.

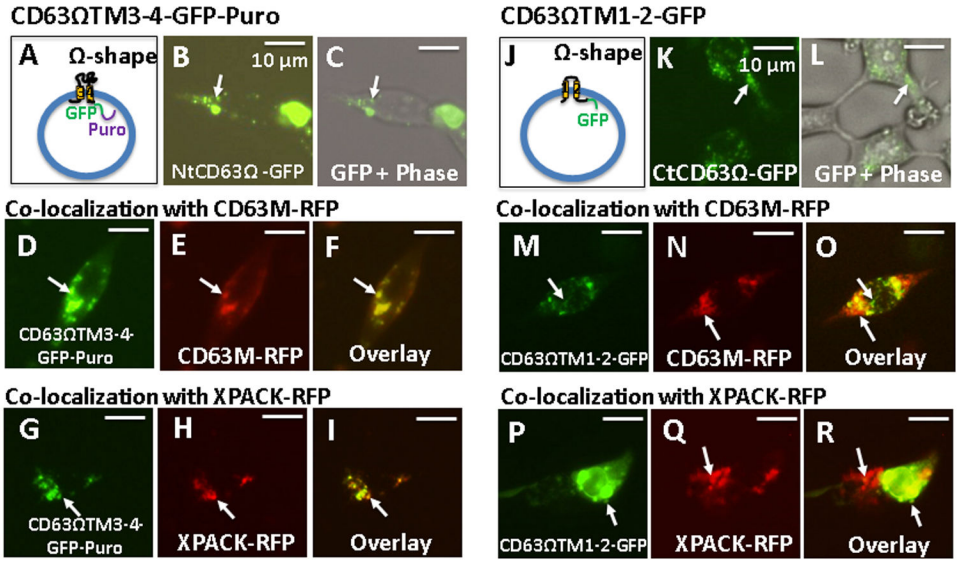

Figure 4. Double transmembrane domain-deleted truncates (CD63ΩTM3-4 and CD63ΩTM1-2) and their subcellular localization in living HEK293 cells.

Cells were transfected with the fusion construct of CD63ΩTM3-4-GFP-Puro (**left panels, A-C**). At 72 hrs, cells exhibited punctuated green fluorescence within their cytosol (**B, C, arrows**). When cells were co-transfected with the full-length CD63M-RFP or the exosome marker, XPACK-RFP, CD63ΩTM3-4 was found to colocalize with both the full-length CD63M-RFP (**D-F**) and XPACK-RFP (**G-I**). In contrast, CD63ΩTM1-2 truncate demonstrates a punctuated cytosolic pattern (**right panels, J-L**). While CD63ΩTM1-2 truncate demonstrates a punctuated cytosolic pattern (**J-L**), there is no significant co-localization with either the full-length CD6M-RFP (**M-O**) or exosome marker XPACK-RFP (**P-R**) in co-transfected cells. Arrows indicate endosome/exosome/MVB structures. Scale bar: 10 μm.

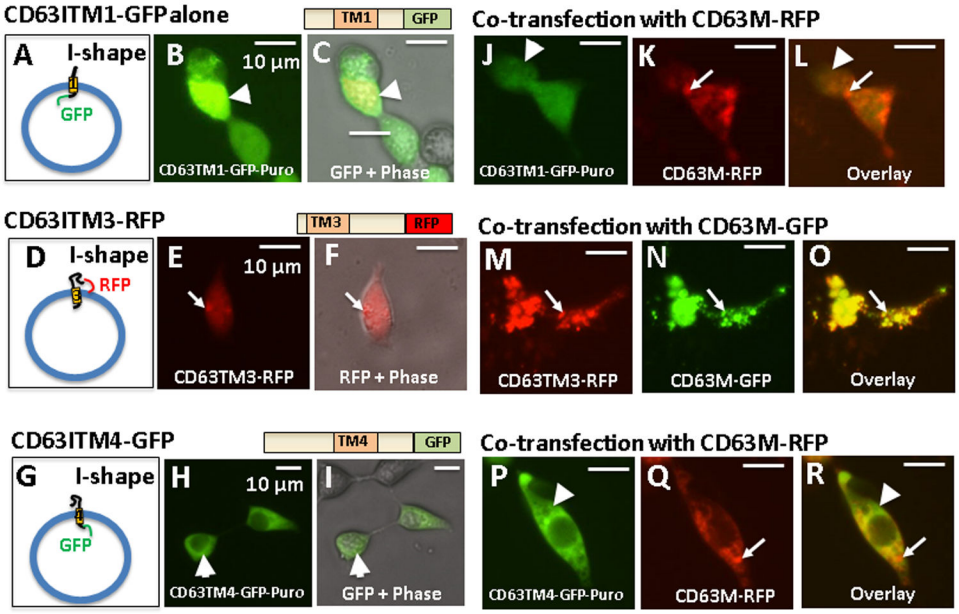

Figure 5. Single transmembrane domain retaining truncates (CD63TM1, CD63TM3, and CD63TM4) and their intracellular localization in living HEK293 cells.

Cells were transfected with I-shape CD63 truncates including either TM1-only (**top panels**), or TM3-only (**middle panels**) or TM4-only (**bottom panels**). At 72 hrs post-transfection, green fluorescent signals were recorded and images showed an even cytosolic distribution for both CD63TM1-GFP-Puro (**A-C**) and CD63TM4-GFP-Puro (**G-I**). In contrast, red fluorescent signal punctuates were recorded for CD63TM3-RFP (**D-F**). In a separate set of experiments, cells are co-transfected with the full-length CD63M along with either CD63TM1 (**J-L**), or CD63TM3 (**M-O**) or CD63TM4 (**P-R**). fluorescent images were recorded 72 hours after co-transfection and showed overlapping of CD63TM3-RFP with CD63M-GFP in a punctated pattern (**O, yellow color**). In contrast, CD63TM1-GFP-Puro (**J-L**) or CD63TM4-GFP-Puro (**P-R**) show no significant overlapping with the red fluorescent signals of the full-length CD63M-RFP, indicated by the appearance of red (thin arrows) and green (thick arrowheads). Scale bar: 10 µm.

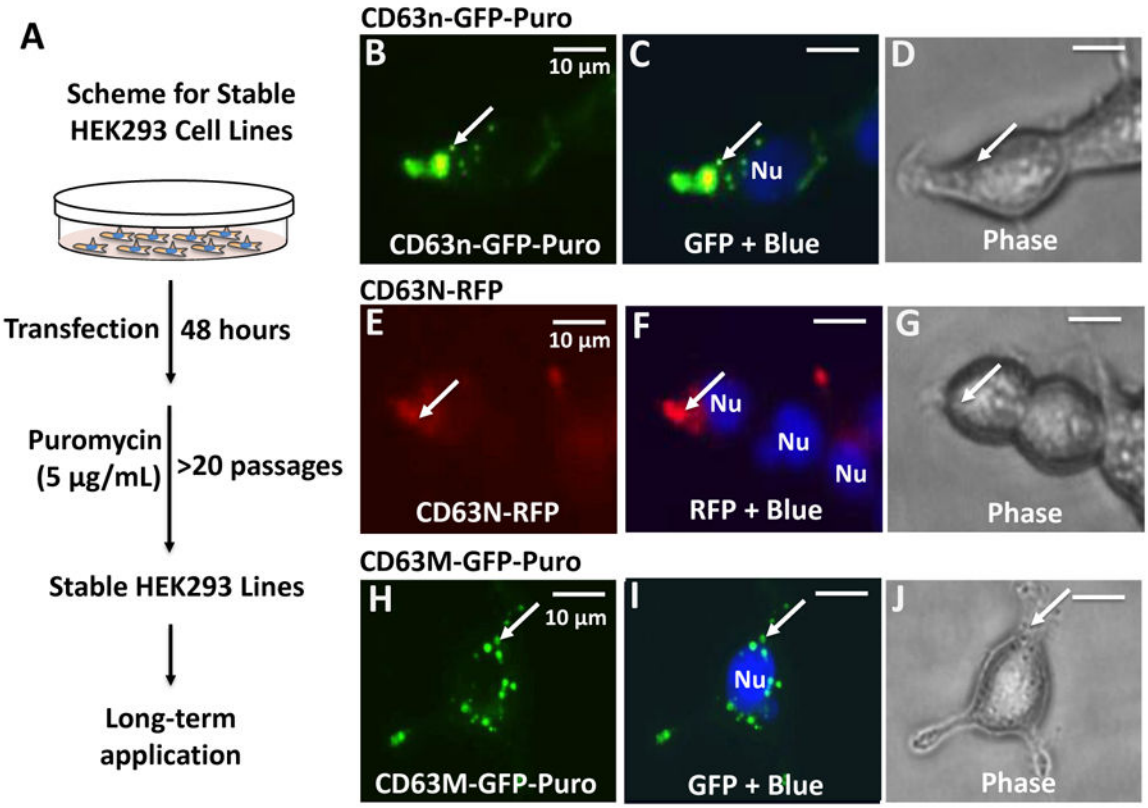

Figure 6. Establishment of stable HEK293 cell lines expressing either full-length CD63 or its terminal domain-deleted variants.

Schematic illustration of experimental procedures for the establishment of stable cell lines (**A**). Stably transfected HEK293 cells (40 days after transfection) expressing either terminal truncate CD63n-GFP-Puro (**B-D, green**) or CD63N-RFP (**E-G, red**) as compared to those of the full-length CD63M-GFP-Puro (**H-J, green**). Stable cells were imaged after 20 passages under puromycin selection. The punctuated cytosolic distribution becomes apparent when the fluorescent images are merged with the blue nuclei stained with HOCHEST (**C, F**, and **I**). The phase images show the corresponding morphology of the imaged cells (**C**, **F**, and **I**). Arrows pointed to expressed chimeric fusion proteins within living HEK293 cells. Scale bar, 10 μm.

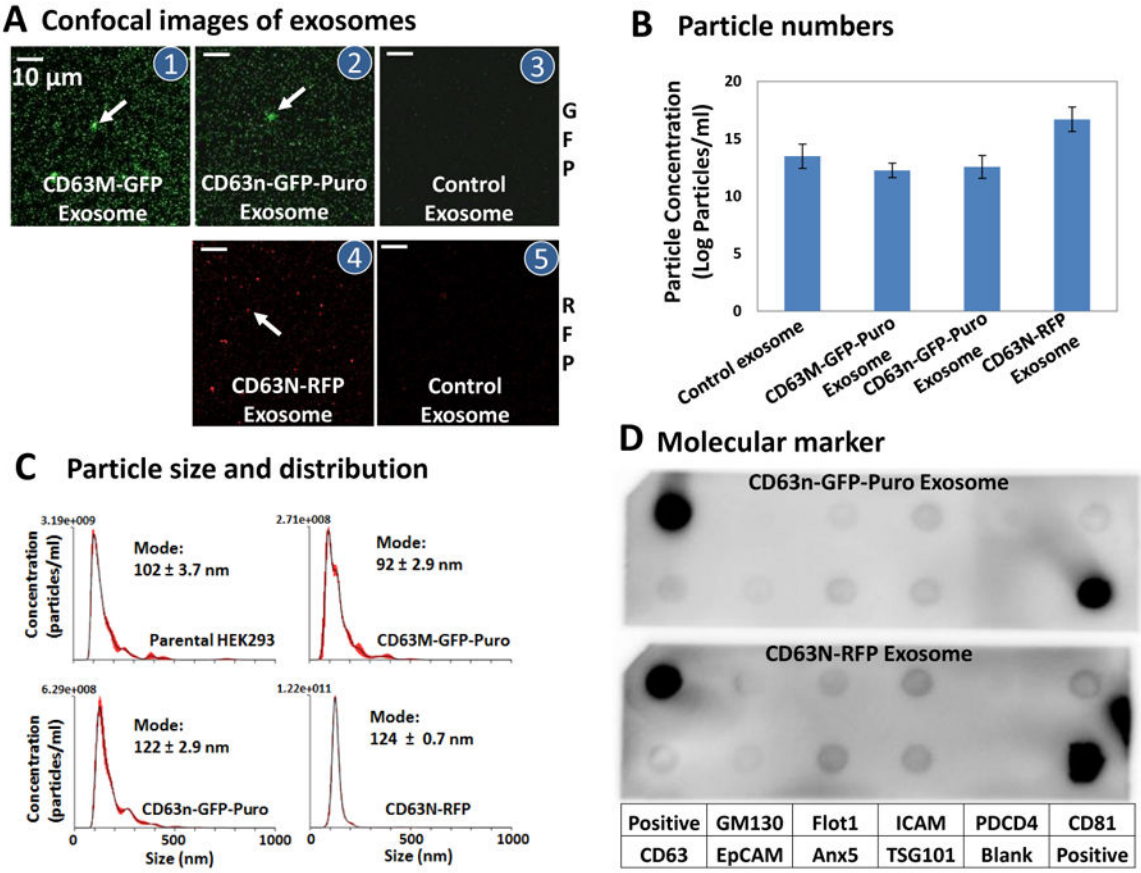

Figure 7. Characterization of engineered CD63-displayed exosomes from the stable HEK293 cells.

Exosome preparations were also subjected to confocal imaging analysis (**A**) particle number quantification via ELISA (**B**), nanoparticle tracking analysis (NTA) for particle size and distribution (**C**), and dot-blot immune-analysis of molecular markers of exosomes. Scale bar: 10 μm.

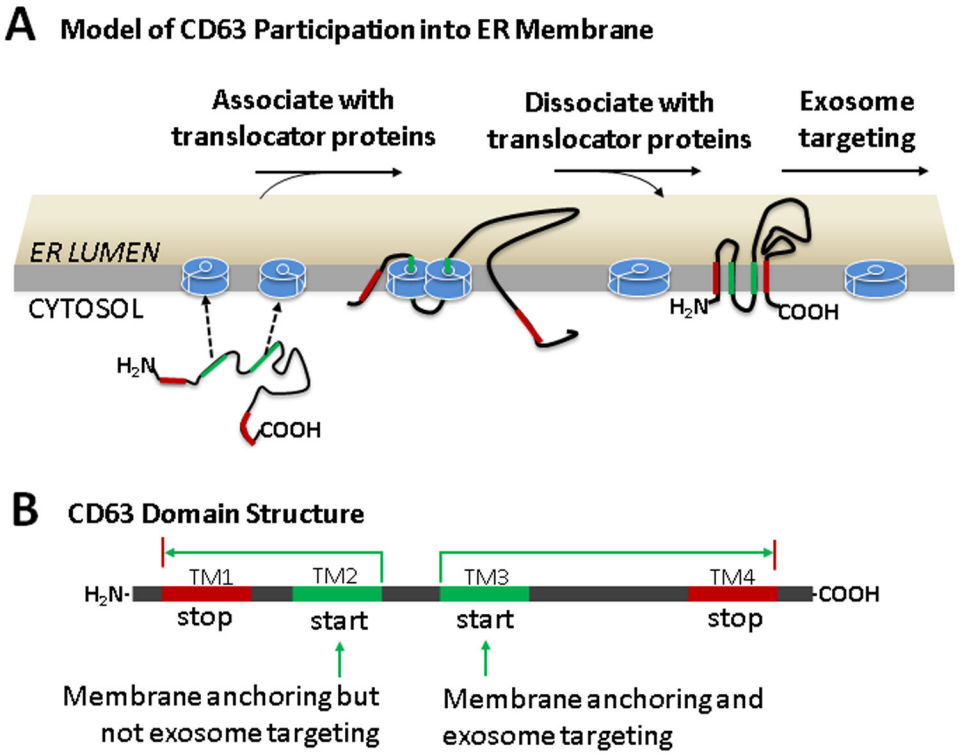

Figure 8. Model of CD63 integration into lipid membrane bilayer in mammalian cells.

(**A**) In the tetraspanin CD63, internal ER signal sequences act as a start-transfer signal and initiates the insertion of the middle potion of CD63 protein either by the transmembrane domain 2 and/or transmembrane domain 3 (TM2 and/or TM3, green). At some point, a stop-transfer sequence (TM1 or TM4, red) enters the translocator, which then discharges the CD63 into the membrane bilayer. This process results in an M-like membrane topology with two free termini situated within the cytosol. (**B**) The transmembrane domain structure of full-length CD63 shows the internal initiation starting domains as well as the stop domains for transmembrane targeting and anchoring.